**DAΦNE TECHNICAL NOTE**

INFN - LNF, Accelerator Division

Frascati, March 7, 1994

Note: **I-12**

# INJECTION CONFIGURATION IN DAΦNE

*S. Guiducci*

## 1. Introduction

Injection into DAΦNE has been already described[1], we recall here the relevant aspects. Injected beam ($e^+$ and $e^-$) comes from a damping ring, and therefore it has small dimensions in phase space, even smaller than those of the DAΦNE beam.

Injection takes place in the straight section of the long part of each ring and the beam comes from the inside in the $e^-$ machine and from the outside in the $e^+$ one.

In the following injection parameters are calculated for the $e^+$ ring, for the $e^-$ ring the opposite sign for the kickers angles has to be taken. Since $e^+$ and $e^-$travel in the same direction in the injection section of their own rings, the magnetic field in the kickers has the same sign.

## 2. Choice of the injection kickers

The kickers configuration for injection into DAΦNE has been optimized for the DAY-ONE lattice D13 [2]. Due to the transparency criterion adopted in the main rings design the injection section, and therefore the kicker angles, is practically the same in all the lattices.

The septum position with respect to the DAΦNE central orbit $x_{septum}$ has been chosen at the limit of the vacuum chamber half aperture $A_x$ required for the stored beam. For good beam lifetime $A_x$ is $10\sigma_x$ plus closed orbit allowance[3]. In the two planes the required beam stay-clear half apertures at the septum locations are:

$$A_x = (29+3)\ \text{mm} = 32\ \text{mm}$$

$$A_y = (13+2)\ \text{mm} = 15\ \text{mm}.$$

The injection parameters are listed in **Table I**.

**Table I - Injection parameters**

| | | | |
|---|---|---|---|
| $x_{septum}$ | 32 mm | $\varepsilon$ | $1.0\ 10^{-6}$ |
| $\Delta x_s$ | 4.2 mm | $\beta_{septum}$ | 8.92 m |
| $x_{bump}$ | 20 mm | $\eta_{septum}$ | 0. |
| $Q_x$ | 5.18 | $\varepsilon_{inj}$ | $2.5\ 10^{-7}$ |
| $Q_y$ | 6.15 | $\beta_{inj}$ | 6m |

The orbit bump is given by:

$$x_{bump} = x_{septum} - 4\sigma_x = 20 \text{ mm}$$

and satisfies with a large margin the condition:

$$x_{bump} > 6\sigma_{xinj} + \Delta x_s = (7.\ 3+ 4.2) \text{ mm} = 11.5 \text{ mm}$$

where $\sigma_x$ , $\sigma_{xinj}$ are the beam dimensions in DAΦNE and in the accumulator respectively and $\Delta x_s$ is the width of the septum.

The optical functions in the injection region are shown in **Fig. 1**. The dispersion function is zero and there are no sextupoles in the region of the orbit bump.

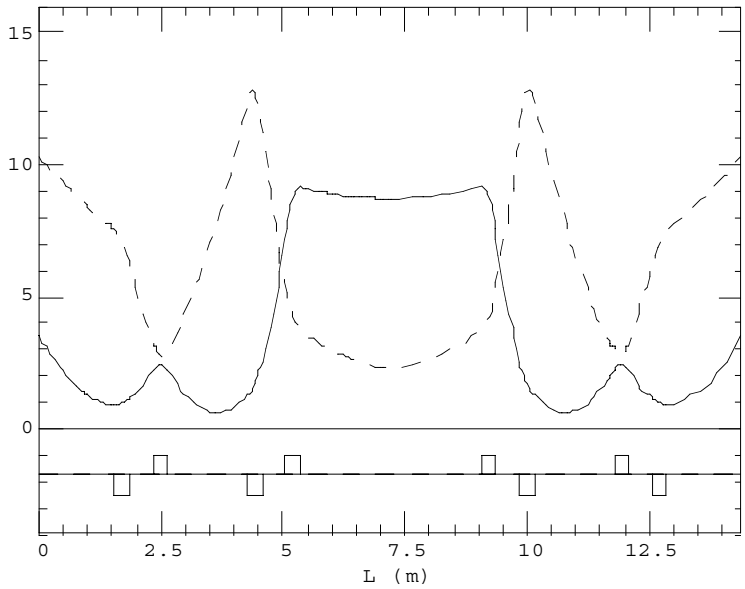


***Fig. 1*** *- Optical functions in the injection straight section.*

Two kickers would be sufficient for injection because they can be placed exactly at $\pi$ distance in phase advance, but this would fix the phase advance in this region. As we want to keep the flexibility of changing the betatron wavenumbers of the ring $Q_x$, $Q_y$ by varying the quadrupole gradients in the injection section we have chosen a configuration with three kickers.

The kickers configurations considered are shown in **Fig. 2a,b**: there is only one kicker to adjust the injected beam coming from the septum and two kickers on the other side to make a closed bump orbit for the stored beam.

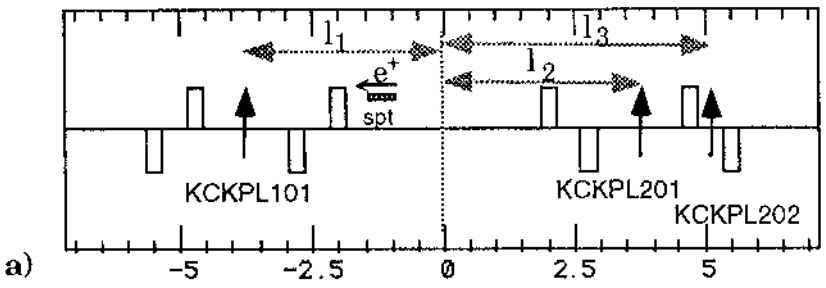


**a1)** $l_2$ = 3.66759 **a2)** $l_2$ = 3.78759

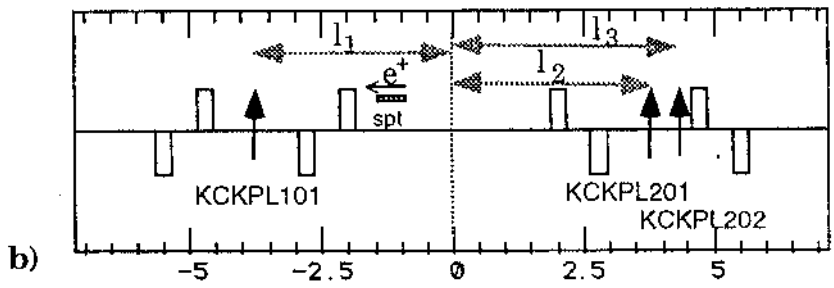


**b1)** $l_2$ = 3.66759m **b2)** $l_2$ = 3.78759m

***Fig. 2*** *- Kickers configurations:* $l_1$ *= 3.78759m* ***a)*** $l_3$ *= 5.10759m;* ***b)*** $l_3$ *= 4.42759m.*

The position of the first kicker (KCKPL101) has been chosen in order to have a phase advance difference with respect to the septum exit as near as possible to $\pi/2$ for an interval of machine tunes around the design value $Q_x$ = 5.18.

The angle $\delta_1$ required by the first kicker to obtain the desired value of the orbit at the septum is given, at different $Q_x$ values, in **Table II**. The value of the angle of the bumped orbit at the septum end is also shown because it is not zero but always very small.

**Table II**

| $Q_x$ (mrad) | $x'_{bump}$ (mrad) | $\delta_1$ |
|---|---|---|
| 5.09 | .21 | 7.94 |
| 5.18 | -.20 | 8.03 |
| 5.22 | .12 | 7.97 |

In **Table III** the angles of the second and third kicker (KCKPL202, KCKPL201), normalized to $\delta_1$, are given for different $Q_x$ values and for two different positions of each kicker.

**Table III**

| | **a)** $l_3$ = 5.10759 | | **b)** $l_3$ = 4.42759 | | $Q_x$ |
|---|---|---|---|---|---|
| | $\delta_2/\delta_1$ | $\delta_3/\delta_1$ | $\delta_2/\delta_1$ | $\delta_3/\delta_1$ | |
| **1)** $l_2$ = 3.66759 m | .79 | .25 | 62 | .33 | 5.09 |
| | 1.04 | 0. | 1.04 | 0. | 5.18 |
| | 1.0 | .05 | .97 | .06 | 5.22 |
| **2)** $l_2$ = 3.78759 m | .86 | .15 | .72 | .23 | 5.09 |
| | 1.13 | -.14 | 1.23 | -.18 | 5.18 |
| | 1.08 | -.09 | 1.15 | -.12 | 5.22 |

Row **1)** of Table III shows a configuration with the second kicker at $\pi$ phase distance from the first one for the design value of $Q_x$ = 5.18. For this $Q_x$ value the third kicker is off and is turned on only when $Q_x$ is varied.

The third kicker can be placed either between the two quadrupoles or in the same section as the second one (see **a1** and **b1** in **Fig. 2**); in the second case the strength is higher.

The solution shown in row **2)** (**a2** and **b2** in **Fig. 2**) of Table III has the second kicker displaced by 12 cm to increase the phase advance distance from the first kicker. In this case the angle of the third kicker changes its sign within the $Q_x$ range considered, but the required integrated field is smaller. This gain in the strength of the third kicker is less than a factor two and the requirement of changing sign makes the power supply more complicated, therefore we have chosen the first solution. Using for the third kicker the same power supply designed for the other two, the required kicker length is 1/3 of the others.

The position of the third kicker is not critical. The configuration **a1**,i.e. the third kicker placed in between the quadrupole doublet, requires a smaller angle but the third kicker can be placed also in the same straight section as the second one (**b1**) if it is convenient to design a single modified vacuum chamber.

The required kicker angles have been calculated, in the **b1** configuration, also for the D15 lattice[2] and are shown in **Table IV**. The difference with respect to the D13 lattice is negligible.

**Table IV**

| | $Q_x$ | $\beta_x$ (m) | $x'_b$(mrad) | $\delta_1$(mrad) | $\delta_2/\delta_1$ | $\delta_3/\delta_1$ |
|---|---|---|---|---|---|---|
| **D13 - b1** | 5.18 | 8.92 | -.20 | 8.03 | 1.04 | 0. |
| **D15 - b1** | 5.18 | 7.57 | -.22 | 8.06 | 1.07 | .02 |

The maximum angle of the kickers is $\delta_2$ = 8.4 mrad corresponding to 142 Gm at 510 MeV. The pulse duration should be **less than one revolution period and equal for the three kickers**.

The required beam stay-clear aperture in the kickers section is [3]:

$$A_x = (14+2) \text{ mm} = 16 \text{ mm}$$
$$A_y = (25+3) \text{ mm} = 28 \text{ mm}.$$

## 3. Tracking simulations

For injection of thirty bunches vertical separation of the beams at the parasitic crossing points is not required. A tracking simulation of the injected beam, with sextupoles on, has been performed for the DAY-ONE lattice. The initial coordinates of the injected beam are chosen by gaussian extraction with the parameters summarized in **Table V** and the kickers configuration **b1** of Fig. 2.

**Table V**

| | | | |
|---|---|---|---|
| $Q_x$ | 5.18 | $Q_y$ | 6.15 |
| $\sigma_x$ (mm) | 1.2 | beam center position: | |
| $\sigma_x'$ (mrad) | .24 | $x_0$(mm) | 40. |
| $\sigma_y$ (mm) | .27 | $x_0'$ (mrad) | .396 |
| $\sigma_y'$ (mrad) | .11 | $y_0$ (mm) | 0. |
| $\sigma_p$ | .001 | $y_{0'}$ (mrad) | 0. |

A plot of the horizontal and vertical phase space at the septum exit is shown in **Fig. 3a,b** with 20 particles tracked for 100 turns. The injection efficiency is 100% and the horizontal oscillation of the beam is well inside the dynamic aperture.

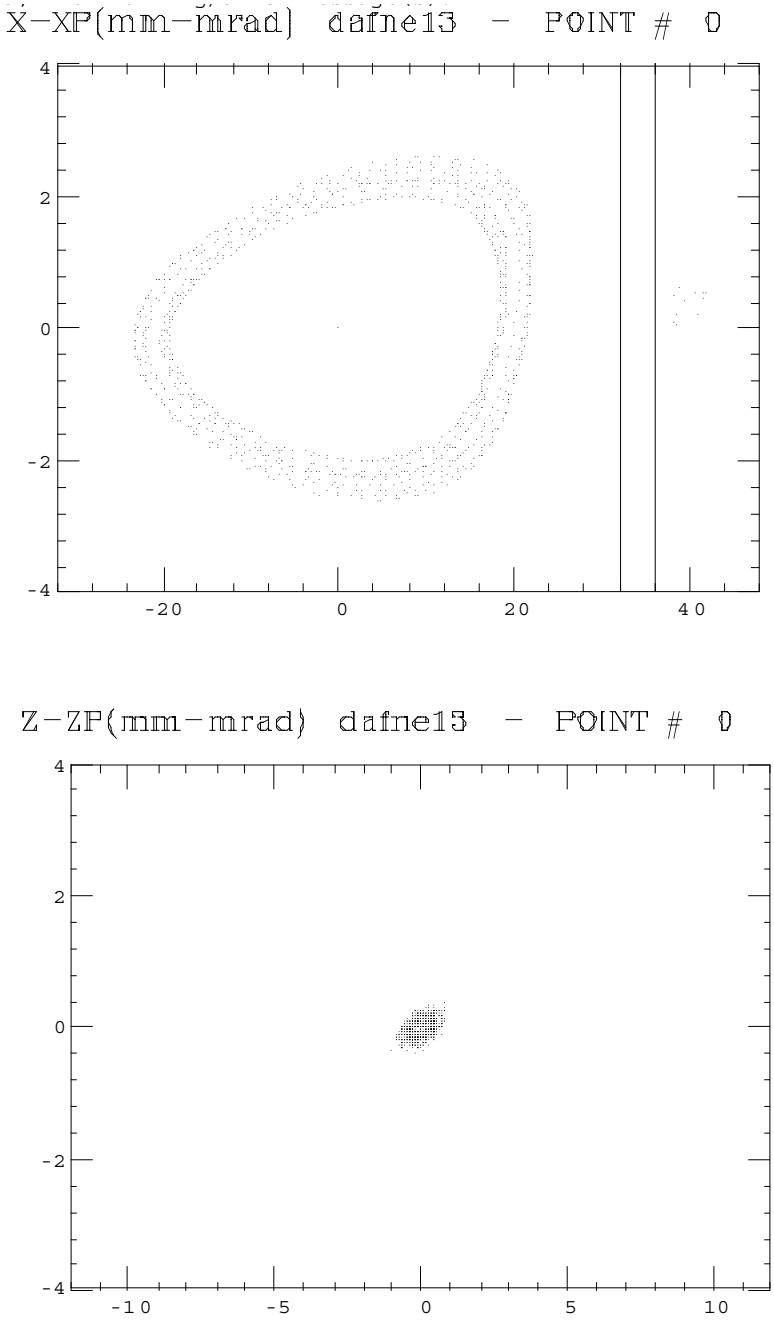


***Fig. 3*** *- Horizontal* ***a)*** *and vertical* ***b)*** *phase space at the septum exit. 20 particles, 100 turns.*

For more than 30 bunches a vertical orbit bump to separate the beams at the parasitic crossings is required. Since there are two sextupoles inside the orbit bump there is a strong coupling of the horizontal and vertical oscillations at injection.

This coupling yields a large increase of the vertical emittance. Tracking has been performed, for the above described injection configuration, with a vertical orbit at IP of 2.5 mm obtained with the correctors strengths listed in **Table VI**.

**Table VI**

| IR1 | | IR2 | |
|---|---|---|---|
| corrector | angle (mrad) | corrector | angle (mrad) |
| CHVPL106 | -5.59 | CHVPS205 | -5.758 |
| CVVPL107 | 4.245 | CVVPS206 | 4.426 |
| CHVI1002 | 2.0 | CHVI2002 | 2.0 |
| CHVI1001 | 2.0 | CHVI2001 | 2.0 |
| CVVPS101 | 4.43 | CVVPL201 | 4.245 |
| CHVPS102 | 5.758 | CHVPL202 | 5.594 |

The Courant-Snyder invariant $W_{x,z}$ for an injected particle, calculated with the linear optical functions at the septum location, is shown in **Fig. 4a,b** as a function of the number of turns.

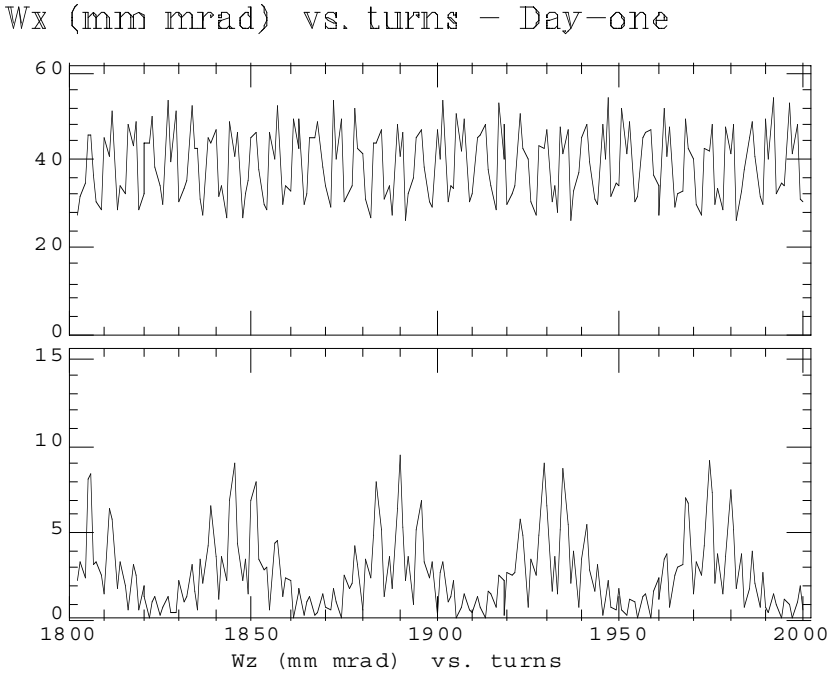


***Fig. 4*** *- $W_x$ and $W_z$ versus the number of turns for an injected particle.*

In presence of sextupoles, for the large oscillations of the injected beam, the phase space ellipse is strongly distorted and the Courant-Snyder invariant changes with time. In Fig. 4 two different oscillation frequencies can be distinguished: the first has a period $N \sim 1/\Delta\nu_{x,z}$ and is due to the deformation, caused by the sextupoles, of the phase space ellipse. The second has a period of ~ 50 turns and is due to the coupling of betatron oscillations.

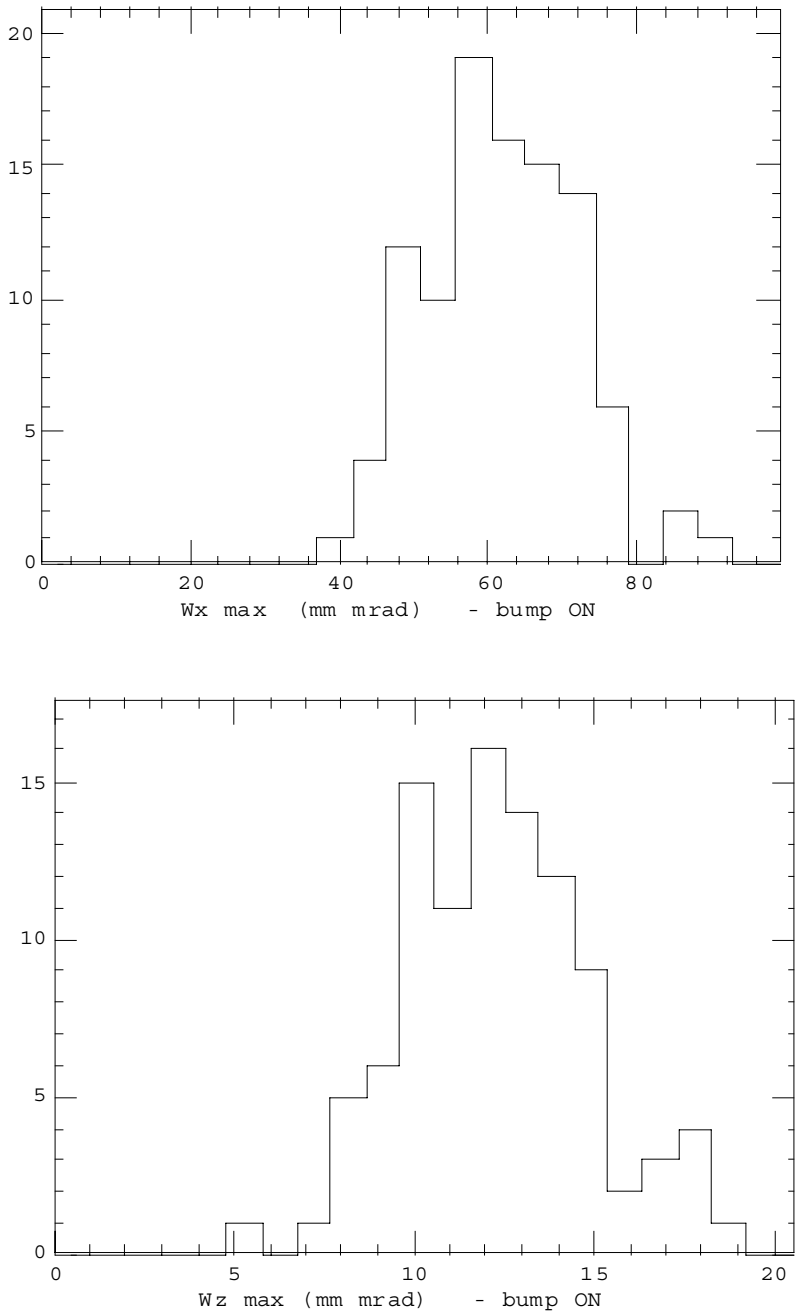


***Fig. 5*** *- Histogram of the maximum invariant over 100 turns with vertical orbit bump at IP.* ***a)*** *Horizontal,* ***b)*** *vertical.*

To see the increase in the vertical emittance, due to the coupling, we have plotted in **Figs. 5a** and **b**, respectively, the histogram of the maximum $\mathbf{W_x}$ and $\mathbf{W_z}$ over 100 turns for 99 particles.

For comparison the same histograms are shown in **Fig. 6a,b** for a tracking with the vertical orbit bump turned off.

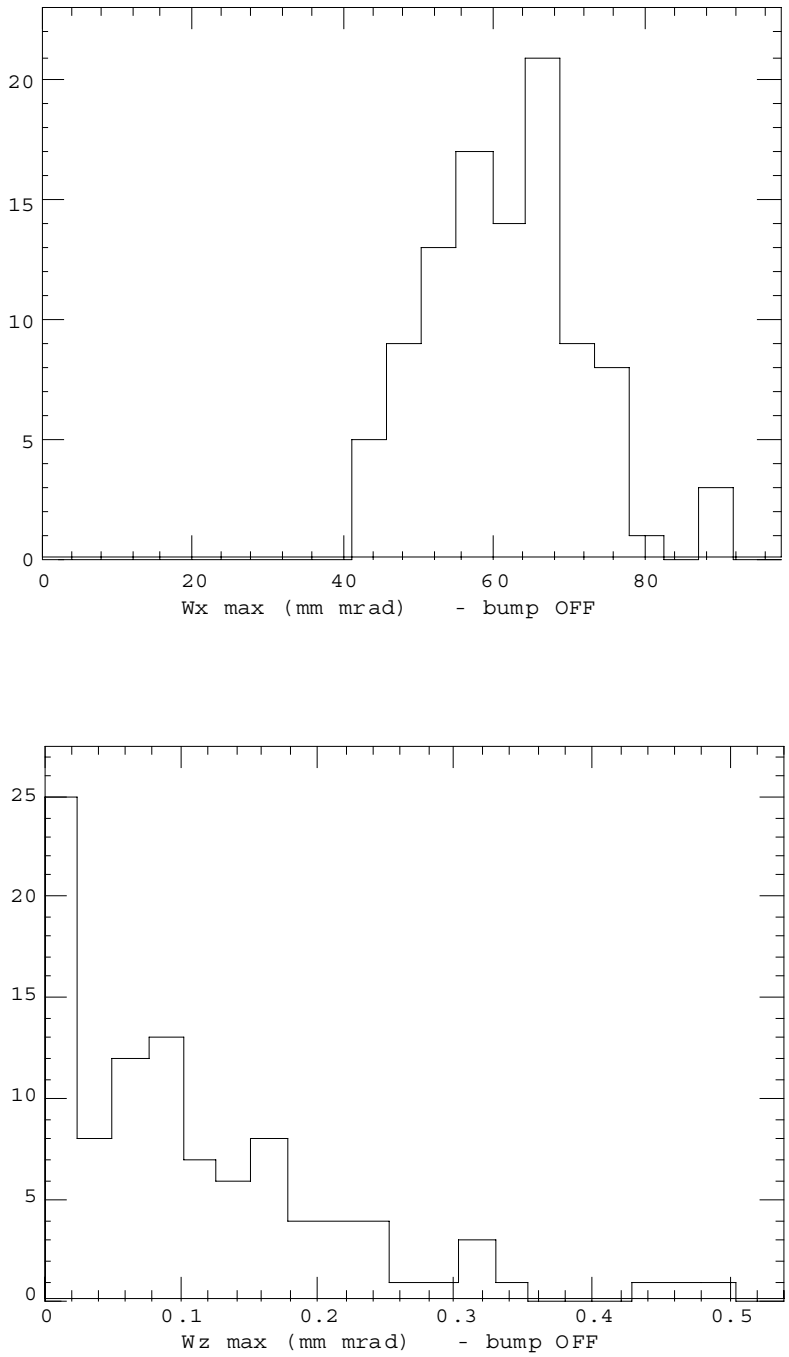


***Fig. 6** - Histogram of the maximum invariant over 100 turns without vertical orbit bump at IP. **a)** Horizontal, **b)** vertical.*

The distribution of $\mathbf{W_x}$ is nearly the same in the two cases; it ranges between 40 and 90 mm mrad with a peak around 60. The horizontal vacuum chamber aperture at the septum corresponds to $W_x$=115 mm mrad.

$\mathbf{W_z}$ is very different, in fact, when the bump is off, the maximum invariant is less than .5 mm mrad ,i.e. less than 1% of the horizontal value. When the bump is on $W_z$ varies between 5 and 20 mm mrad, with a peak around 12, i.e. it is $W_z \sim \frac{1}{4} W_x$, which is large but well inside the vacuum chamber aperture corresponding to 50 mm mrad.

Due to this coupling effect, the vertical beam size at the parasitic crossings is larger than the beam separation given by the orbit bump and makes it ineffective. The problem of the parasitic crossings for injection of more than 30 bunches requires a further analisys and has to be studied running a simulation code[4]. If the vertical separation of the beams at the parasitic crossings is realy needed a solution to this problem might be the design of an injection lattice without any sextupole inside the vertical orbit bump.

The maximum over the last 200 turns of the vertical invariant for 20 particles has been computed tracking for a different number of turns from 200 to 2000 to see if there is a diffusion process. Increasing the number of turns there is a slight modulation of the maximum of $W_z$ but no continuous growing.

## 4. Conclusions

For phase I (30 bunches) injection into DAΦNE is feasible with the low-$\beta$ lattice and highly efficient because the injected beam comes from a damping ring and therefore has very small sizes, the vacuum chamber is quite large and the injection section is specially designed.

For phase II (injection of up to 120 bunches) the need of a vertical separation at the parasitic crossing has to be further investigated by means of a weak-strong beam-beam simulation. If there are injection configurations which require the vertical separation and the coupling between the vertical and horizontal oscillations makes it ineffective a different injection lattice, without sextupoles in the vertical orbit bump, has to be designed.

## References

[1] "Injection into DAΦNE and timing requirements for the linac-accumulator-main ring complex", Technical note I-6, M. Preger.

[2] "Review of DAΦNE lattices", Technical note L-9, M.E. Biagini. C. Biscari, S. Guiducci, M.R. Masullo, X. Lu, G. Vignola.

[3] "DAΦNE stay-clear apertures", Technical note L-6, C. Biscari.

[4] "Beam-beam interactions with parasitic crossings", DAΦNE 3rd machine review,july 7-9,1992, M.Bassetti,C. Biscari.